



HAL
open science

Optical response of heterogeneous layer containing silver nanoparticles

Miriam Carlberg, Florent Pourcin, Olivier Margeat, Judikaël Le Rouzo, Gérard Berginc, Rose-Marie Sauvage, Jörg Ackermann, Ludovic Escoubas

► **To cite this version:**

Miriam Carlberg, Florent Pourcin, Olivier Margeat, Judikaël Le Rouzo, Gérard Berginc, et al.. Optical response of heterogeneous layer containing silver nanoparticles. *Beilstein Journal of Nanotechnology*, 2017, 8, pp.1065 - 1072. 10.3762/bjnano.8.108 . hal-01788938

HAL Id: hal-01788938

<https://amu.hal.science/hal-01788938v1>

Submitted on 9 May 2018

HAL is a multi-disciplinary open access archive for the deposit and dissemination of scientific research documents, whether they are published or not. The documents may come from teaching and research institutions in France or abroad, or from public or private research centers.

L'archive ouverte pluridisciplinaire **HAL**, est destinée au dépôt et à la diffusion de documents scientifiques de niveau recherche, publiés ou non, émanant des établissements d'enseignement et de recherche français ou étrangers, des laboratoires publics ou privés.

Optical response of heterogeneous layer containing silver nanoparticles

Miriam Carlberg¹, Florent Pourcin², Olivier Margeat², Judikaël Le Rouzo^{1,*}, Gérard Berginc³, Rose-Marie Sauvage⁴, Jörg Ackermann² and Ludovic Escoubas¹

Address: ¹Aix Marseille Univ, Université de Toulon, CNRS, IM2NP, Marseille, France and ²Aix Marseille Univ, CNRS, CINaM, Marseille, France and ³Thales Optronics, Elancourt, France and ⁴DGA/DS/MRIS, 75015 Paris, France

Email: Judikaël Le Rouzo – judikael.lerouzo@im2np.fr

* Corresponding author

Abstract

Metal nanoparticles are of considerable interest in various domains ranging from biology to chemistry or medicine. In physics, the field of light matter interaction is specially challenging. Our work is focused on the optical properties of silver nanostructures enclosed in a polymer host matrix. Their introduction in polymer thin films is assumed to result in layers with adaptable optical properties. Thin film layers with inclusions of differently shaped particles, such as nanospheres and nanoprisms, and of different sizes, are optically characterized.

Nanoparticles are produced by simple chemical synthesis at room temperature in water. The plasmonic resonance peaks of the different colloidal solutions range from 390 to 1300 nm.

The non-absorbing and transparent polymer matrix chosen is polyvinyl pyrrolidone because of its optical and chemical properties. The optical studies of the layers include spectrophotometry and spectroscopic ellipsometry measurements, which result in knowledge of the reflection, the transmission, the absorption and the complex optical indices n and k . Finite difference time domain simulations of nanoparticles in thin film layers allow the visualizations of the particle interactions or the electric field enhancement on and around the particles to complete the optical characterizations.

A simple analysis method is proposed to obtain the complex refractive index of nanospheres in polymer and nanoprisms in polymer.

Keywords

Plasmonic nanoparticles; nanospheres; nanoprisms; spectroscopic ellipsometry; thin film layers

Introduction

Noble metal nanoparticles (NP) are of considerable interest in various domains ranging from chemistry to medicine or light filtering [1–6]. Silver NP are especially challenging because of the possibility to control the phenomenon of light matter interaction in the visible wavelength range. Optical properties of these metallic NP are induced by localized surface plasmon resonances, which are size, shape, material and environment dependent [7]. At the localized surface plasmon resonance wavelengths, the conduction electrons of the NP oscillate coherently, which induces an electric field enhancement. The incoming light is either absorbed or scattered by

the NP [8]. The absorption and scattering are commonly referred to as optical extinction. Single NP are widely studied under different characterization techniques and computer modeling, such as Mie theory for spherical NP. The absorption dominates the extinction for small radii and scattering for larger radii. For silver, the threshold radius is 20 nm [9].

Following these properties, the optical properties of the thin films can be chosen by embedding specifically designed NP. Especially, by choosing silver NP the thin film layers will absorb in the visible wavelength range. This leads to applications of plasmonic thin film layers for photodetectors [10], photovoltaics [6,11] or non-reflecting coatings [12–14].

Silver NP were chosen for their high electric field enhancement in the visible wavelength range [15]. Progress in the chemistry of NP synthesis allowed us to choose a chemical process adapted to our study that produces NP of different shapes and sizes. Among different NP production methods, chemical synthesis is easy to implement and produces NP at low costs. Standard physical vapor deposition methods require high energy sources, such as lasers [16], whereas chemical synthesis produces, among other shapes, nanospheres and nanoprisms of different sizes in water at room temperature. Taking advantage of these size and shape versatility of chemical synthesis, we aim to control the absorption of thin film layer by embedding different NP.

When included in polymer thin film layers such as polyvinyl pyrrolidone (PVP), the plasmon resonance wavelengths of the NP are red-shifted with respect to the resonance wavelengths in water. This environment dependence can easily be understood by considering the absorption cross-section σ_{abs} variation of a spherical NP according to the Mie theory:

$$S_{abs} = 4\rho k r^3 \text{Im}\left(\frac{\epsilon - \epsilon_m}{\epsilon + 2\epsilon_m}\right) \quad (1)$$

where k is the wave vector, ϵ is the complex dielectric function of the NP and ϵ_m the complex dielectric function of the surrounding medium. Furthermore, collective resonances can alter the optical properties of these NP and further redshift the absorption peaks.

In the following we present studies of thin film layers with differently shaped and sized silver NP inclusions. The NP are obtained by a facile water-based chemical synthesis at room temperature [17,18]. Depending on the chosen reagents, different shapes are achieved. To cover the whole visible wavelength range, we synthesized nanospheres and nanoprisms as their colloidal solutions absorb from 390 up to 1300 nm. The nature of the absorption peak was determined through spectrophotometer measurements coupled with computer simulations and Transmission Electron Microscopy (TEM) imaging. Spectrophotometer and spectroscopic ellipsometry measurements of the PVP host matrix validated its non-absorbing and transparent properties. Spectroscopic ellipsometry measurements of the heterogeneous layers of nanospheres and nanoprisms embedded in the host matrix were fitted by the mathematical addition of a Cauchy law and a single Lorentz law centered at the dipolar resonance wavelength of the nanoparticles. Spectroscopic ellipsometry has been previously performed on nanoparticles embedded in dielectrics [19,20], but the nanoparticles were primarily spherical or ellipsoidal. We propose here a simple analysis of nanoprisms based on the analysis of nanospheres in PVP.

Results and Discussion

Characterization of the colloidal nanoparticle solution

The NP are synthesized as described below in the Experimental section. As synthesized, the nanospheres and nanoprisms were at first dispersed in water. The growth of the nanoprisms was fulfilled in two steps: first spherical seeds with specific crystallographic defects were produced and secondly the growth took place on these defects to form nanoprisms [18,21,22]. The absorption of the colloidal solutions of the first and second step, seeds and prisms, (**Figure 1**, a), shows the characteristic plasmonic absorption peaks. The peaks 1 and 1' were identified as the dipolar resonances of the nanoprisms and the nanospheres respectively. The dipolar resonance of the nanoprisms induced an absorption of light between 540 and 750 nm. The width of this absorption was not due to a distribution in size of the NP, but rather to the random orientation of the NP in the solution. Furthermore, Finite Difference Time Domain (FDTD) simulations show that the maximum electric field enhancement (**Figure 1**, b) for p- and s-polarized light do not occur at the same wavelength. For a single nanoprism 50 nm edge size and 10 nm thickness in water, the maximum electric field enhancement for p-polarized light, corresponding to the dipolar resonance wavelength, occurs at 625 nm, whereas the maximum electric field enhancement for s-polarized light occurs at 619 nm.

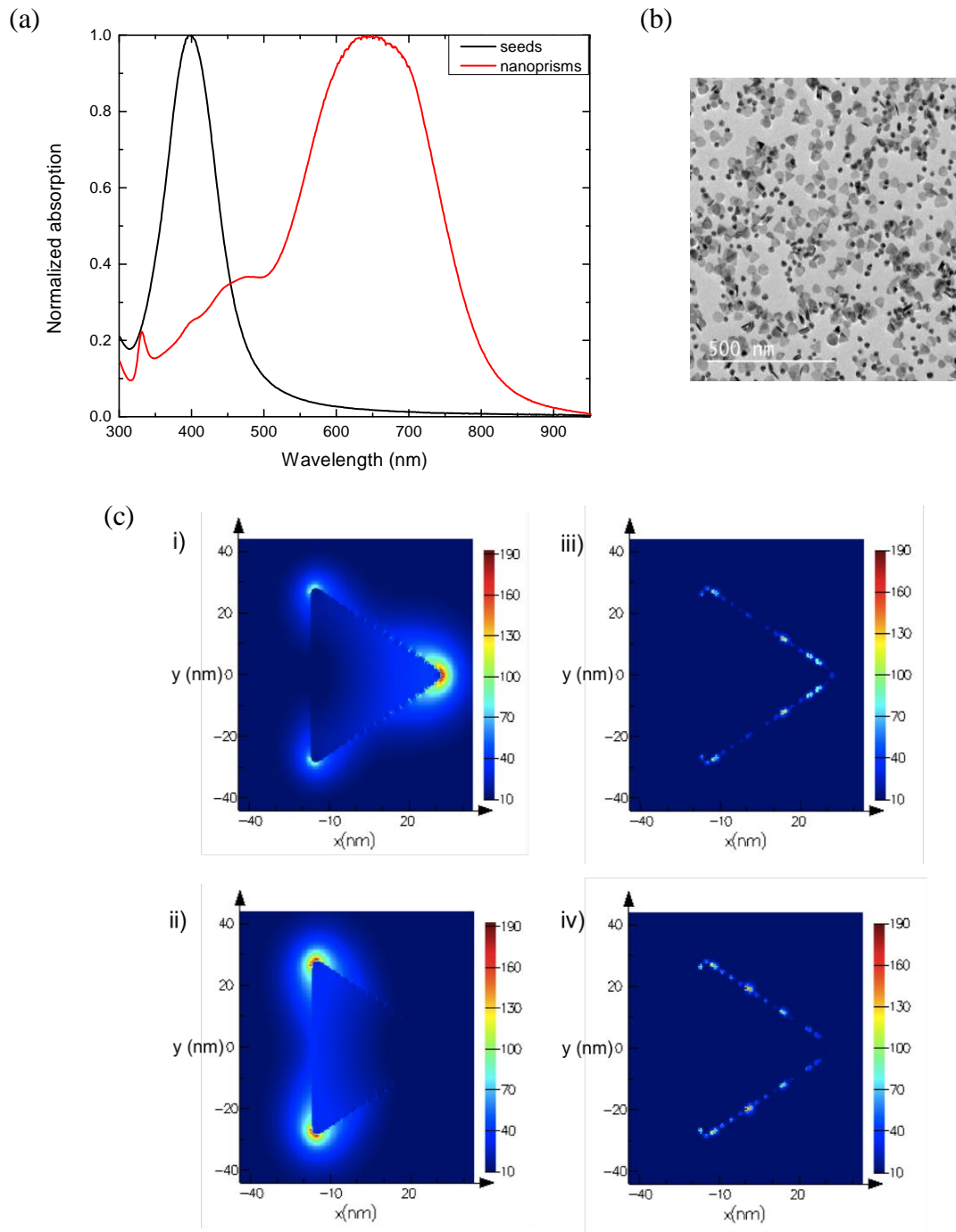


Figure 1: a) Normalized absorption of nanospheres and nanoprisms solutions and b) visualization of the electric field enhancement normalized to the incident electric field in the nanoprism for wavelength of peak 1 under z-oriented p-polarized light (i) and s-polarized light (ii) and for the wavelength of peak 2 under p-polarized light (iii) and s-polarized light (iv).

This absorption peak can be displaced at will in the visible wavelength range by changing the size of the nanoprisms. This is simply done by changing the quantity of seeds added during the second step of the nanoprisms synthesis. The spherical seeds absorbed light between 350 and 430 nm. The nature of the resonances was verified by computer calculations using the Mie theory for the spherical seeds and FDTD for the non-spherical particles. The maximum electric field enhancement for p- and s-polarized light for the dipolar and quadrupolar excitations are pictured on **Figure 1b**. Peak 2 was identified as the quadrupolar resonance peak of the nanoprisms. The absorption peak 3 was supposed to be due to the dipolar resonances of the residual seeds in the nanoprisms solution from the absorption spectrum. TEM images of the NP in solutions confirmed that residual spheres are present.

These different plasmonic resonance peaks presented in the absorption spectrum of the NP in solution, resulted mathematically in the addition of Lorentz functions centered at the different energies.

In summary, silver NP absorbing through the whole visible wavelength range were synthesized and the nature of the absorption peak of the colloidal solution was determined and their optical responses in thin film layers was studied.

Spectroscopic ellipsometry

Spectroscopic ellipsometry is a powerful technique to determine the effective optical indices, real and imaginary parts, of thin film layers or the thickness of known

materials. Indeed, the thickness and the optical indices of the thin film layer are coupled parameters and cannot be obtained simultaneously. To obtain the real and imaginary part of the optical indices of the thin films, variable angle spectroscopic ellipsometry¹⁰ (VASE) measurements were performed with a Semilab rotating compensator ellipsometer. The incident beam was focused on a microspot diameter of the sample (about 100 μm). We measured the polarization change of light upon reflection on a sample in the visible wavelength range, at which the silver NP absorb, from 350 to 950 nm at incident angles of 65°, 70°, 71°, 72°, 73°, 74° and 75°. This polarization change depended on the amplitude and phase variations of the electric fields for p- and s-polarizations. More details on spectroscopic ellipsometry can be found in textbooks [23,24].

For data analysis, the films were considered as an effective medium having properties including the ones of the NP and of the polymer, as has been already reported [19,20,25,26]. The optical modeling was developed using SEA (WinElli3) software. This software uses the Levenberg–Marquardt algorithm [27] to minimize the mean squared error (MSE) between the measured and calculated ellipsometric data ψ and D . To verify the validity of our mathematical model, transfer matrix method¹² (TMM) calculations of the reflectance were compared with reflectance measurements carried out on a spectrophotometer (Lambda 950, PerkinElmer).

It should be noted that the complex refractive index \tilde{n} is $\tilde{n} = n + ik$ where n is the frequency dependent real refractive index and k is the frequency dependent extinction coefficient.

PVP host matrix

To maximize the influence of nanospheres and nanoprisms on the light interaction, the host matrix of the NP has to be a transparent and non-absorbing

polymer in the visible wavelength range. Furthermore, the matrix should be a mild environment for the NP and help the adherence of the NP to the substrate [28]. PVP is commonly used to stabilize silver NP [29,30]. PVP is also a flexible polymer [31]. Integrating plasmonic properties in this flexible matrix can be interesting for flexible devices.

First, the polymer alone was studied. To obtain a complete understanding of the host matrix, PVP of different molar weights, 40,000 g.mol⁻¹ and 55,000 g.mol⁻¹, were deposited in thin film layers. In order to determine the optical indices of the films, in dependence of the molar weight, a dispersion model composed of a Cauchy mathematical law was used for each sample:

$$n(l) = n_{\infty} + \frac{B}{l^2} + \frac{C}{l^4} \quad (2)$$

where n is the refractive index varying with the wavelength, n_∞ is the refractive index at infinite energy, B and C are two constants. The extinction coefficient of the host matrix is zero in the visible wavelength range, i.e. the absorption of the heterogeneous thin films will be only due to plasmonic effects.

The parameters for the Cauchy law are listed in **table 1**. The measured refractive indices (**Figure 2**) indicate a dependence to the molar weight. With increasing molar weight, the material fraction in the layer augmented, leading to a higher refractive index. The choice of the molar weight has therefore an importance when considering the optical properties of the thin film layers.

Table 1: Fitting parameters of spectroscopic ellipsometry measurements for different structures

Sample	Laws	Cauchy parameters	Lorentz parameters

PVP 40,000 g.mol ⁻¹	Cauchy	B=0.0053 μm ² , C=0 μm ⁴	
PVP 55,000 g.mol ⁻¹	Cauchy	B=0.00709 μm ² , C=0 μm ⁴	
PVP 55,000 g.mol ⁻¹ + 20 nm nanospheres	Cauchy + 1 Lorentz	B=0.00544 μm ² , C=0 μm ⁴ , n _∞ =1.57	f=0.005, E ₀ =3.09 eV, Γ=0.41 eV, e _∅ =0.0002
PVP 55,000 g.mol ⁻¹ + 25 nm nanoprisms	Cauchy + 1 Lorentz	B=0.00502 μm ² , C=0 μm ⁴ , n _∞ =1.56	f=0.003 E ₀ =1.9 eV, Γ=0.32 eV, e _∅ =0.0066

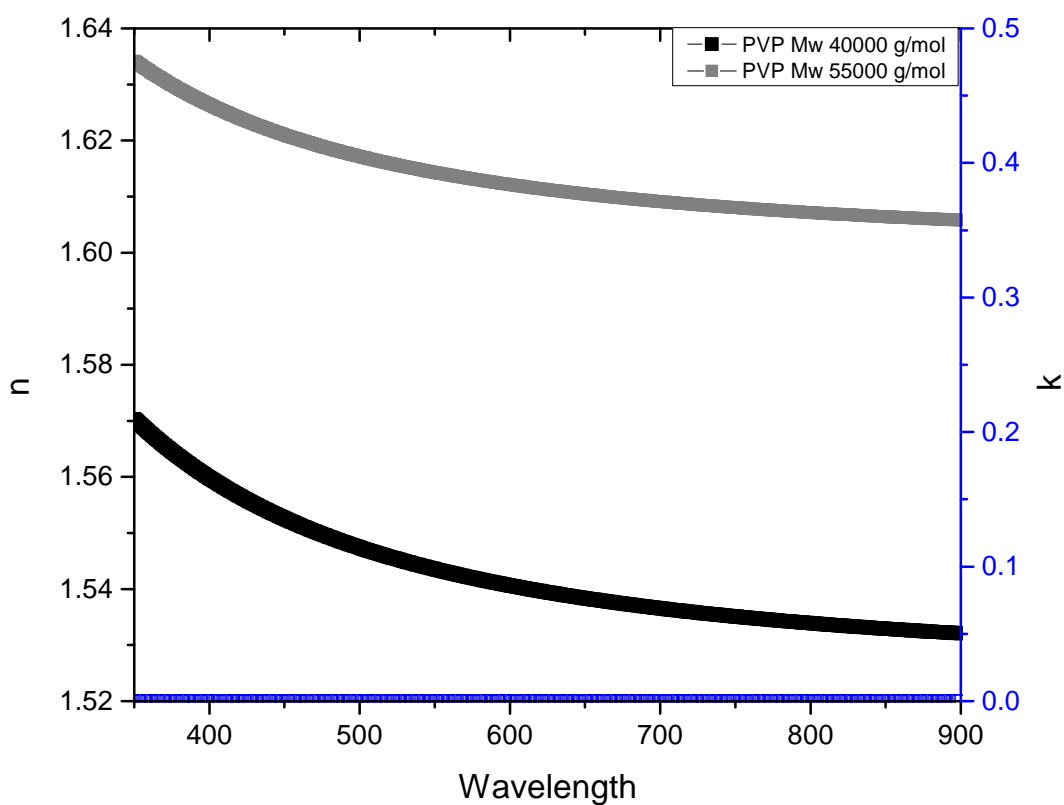


Figure 2: Real and imaginary optical indices of PVP of 40,000 and 55,000 g.mol⁻¹ average molar weight, fitted by a non-absorbing Cauchy law.

In the following, the PVP of molar weight 55,000 g.mol⁻¹ will be chosen for experimental reasons.

Taken together, the host matrix was characterized by spectroscopic ellipsometry and fitted by a non-absorbing Cauchy law. The absorption of the thin film layer derived from the presence of the silver NP.

Heterogeneous thin film layers

By embedding NP into the non-absorbing polymer host matrix they induced absorption of light at their specific plasmonic wavelength resonances. In order to determine the optical indices of the films containing NP, the thin film layer is visualized as an effective medium [32–36]. A dispersion model composed of a non-absorbing Cauchy mathematical law and one or more Lorentz mathematical laws was used.

The Lorentz oscillator model is derived from the classical theory of interaction between light and matter [27]. As it describes the dipolar frequency-dependent polarization due to bound charges, it represents well the plasmonic behavior of metal NP. The Lorentz model influences both the real and imaginary part of the dielectric function:

$$e_1(E) = e_{\infty} + \frac{fE_0^2(E_0^2 - E^2)}{(E_0^2 - E^2)^2 + G^2E^2}, \quad e_2(E) = \frac{fE_0^2GE}{(E_0^2 - E^2)^2 + G^2E^2} \quad (3)$$

where f is the oscillator strength, E_0 in eV is the resonant energy of the oscillator, G in eV is the broadening of the oscillator and e_{∞} is the high energy dielectric constant.

We focused on the plasmonic properties of the silver NP in the visible wavelength range. Therefore, the Lorentz model was sufficient to account for the optical properties of the NP and the electronic intraband transitions occurring in the UV [27] were not considered in this study. The resonant energy and the broadening width of the oscillator were deduced from the absorption energy of the NP. The oscillator strength was the only parameter varied as function of the size and shape of the embedded NP.

By a mathematical addition of the Cauchy and the Lorentz laws, we noticed that the two constants n_∞ , from the Cauchy model, and e_{p} , from the Lorentz model, are only contained in the real part of the dielectric constant and correspond to an offset.

Nanospheres of 10 nm diameter were included in a 55,000 g.mol⁻¹ PVP layer on a silicon substrate. Spectrophotometric measurements indicated that these nanospheres in PVP absorbed at 405 nm, i.e. the oscillator in the Lorentz model was centered at an energy of 3.06 eV. The thickness of the thin film layer, determined by mechanical stylus profilometer (Brucker Decktak XT), was 190±5 nm. The fitting parameters are summarized in **table 1**.

Nanoprisms of 25 nm edge size were deposited in a 55,000 g/mol PVP layer. Their absorption in the PVP layer was centered at 650 nm or 1.9 eV. The thin film layer thickness was 230±5 nm. To fit the data, the Cauchy parameter B was varied. The introduction of the silver NP reduces the amount of PVP, therefore the value of B was affected in comparison with the fit parameters of the PVP layer alone. The parameters of the Lorentz law E_0 and Γ were fixed by the knowledge of the dipolar absorption peak wavelength of the corresponding NP in PVP. The strength of the oscillator was varied in function of the NP density in the thin film layer.

Surprisingly, the nanoprisms were modeled with only one Lorentz law, accounting for the dipolar plasmonic resonance at 700 nm. Adding a second Lorentz law accounting for the quadrupolar resonances of the prisms did not improve the fitting. The second law increases the number of variables from six to nine, but the RMSE did not decrease and the correlation coefficient R^2 did not increase. This leads to the question whether the shape has an influence on the optical indices of the heterogeneous layers or only the size. According to the above samples, only the size has an influence and a single Lorentz law models the plasmonics signature of the NP.

The fit on the nanospheres in PVP sample is optimized up to a $R^2=99.45\%$ and a RMSE=2.1, and the fit on the nanoprisms in PVP sample up to $R^2=99.44\%$ and RMSE=1.9. The obtained optical indices were then used to calculate the reflectance through a TMM calculation. The calculated reflectance was compared to the measured reflectance (**Figure 3**), in order to validate the mathematical laws used to model the thin film layer.

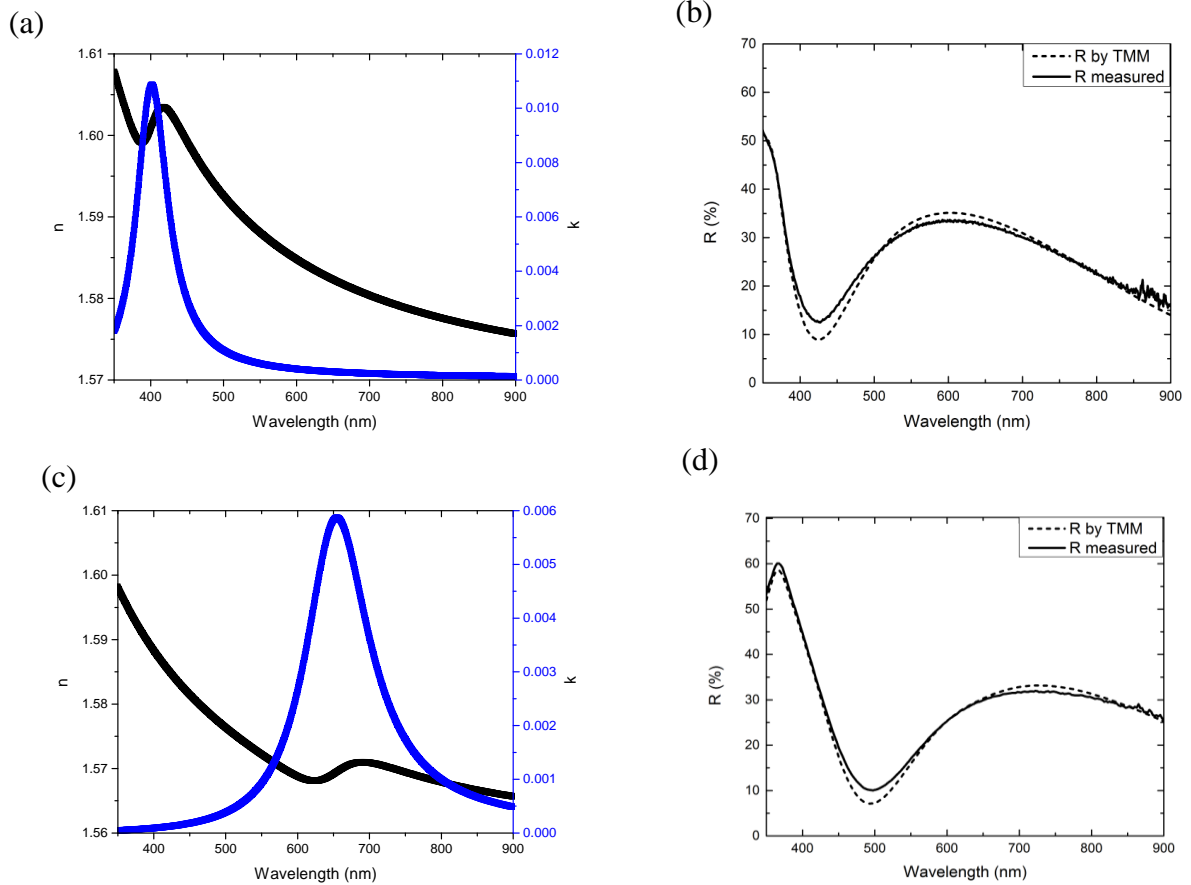


Figure 3: (a) Optical indices n and k and (b) reflectance measured and calculated by TMM for heterogeneous layers with nanospheres and (c) optical indices and (d) reflectance measured and calculated for heterogeneous layers with nanoprisms.

The fit quality being optimized, the comparison between the measured and calculated reflectance is necessary to verify the physical validity of the fit. The two curves follow the same tendencies. The slight discrepancies in the reflectance spectra could be attributed to the measurement or to diffusion phenomena induced by the NP, which is not taken into account in our ellipsometry model.

In summary, the complex optical index of silver nanospheres and nanoprisms embedded in a transparent and non-absorbing polymer layer were modeled by a

mathematical addition of a Cauchy law, accounting for the optical property of the polymer and a Lorentz law, centered at the dipolar absorption wavelength of the embedded NP. The addition of further Lorentz law accounting for higher order resonances or intraband transitions occurring in the UV did not improve the data fit for this specific density of nanoprisms. Further Lorentz laws might be necessary to account for other absorption peaks when the density of nanoparticles in the thin film layer is increased.

Conclusion

In conclusion, chemically synthesized nanospheres and nanoprisms were embedded in a transparent and non-absorbing PVP layer. Spectroscopic ellipsometry measurements were fitted with a mathematical addition of a Cauchy law and one Lorentz law. This easy method allows us to get the optical indices of thin films with complex inclusions. The question arising from these results is whether the shape of the NP matters when embedded in a thin film layer. Further studies with additional shapes of NP will be required to generalize our results, i.e. that only the size matters. A precise knowledge of the morphology of our structures, through AFM or TEM studies may improve our optical models.

Experimental

Synthesis of nanoparticles

NP were synthesized by reduction of silver ions by sodium borohydride at room temperature in water. Nanospheres were synthesized in a one-step method [17]. Nanoprisms were created in a two-step seed-based method [18]. By depositing the

nanospheres directly onto the substrate, their size is determined by atomic force microscopy (AFM), **Figure 4**.

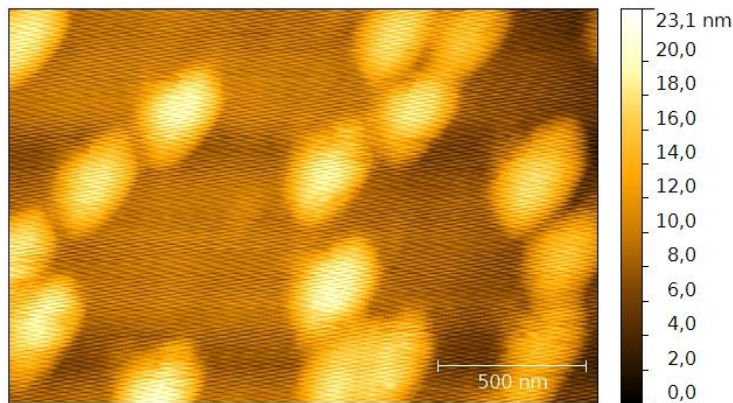


Figure 4: AFM topography of nanospheres on a substrate

The synthesized nanospheres have a diameter of 20 nm. The nanoprisms were equilateral and their edge size varied from 10 to 100 nm depending on the quantity of seed taken in the second step of the synthesis [18,37]. Their thickness was constant 10 nm. The NP were stabilized by citrates and PVP. The colloidal solutions were washed by successive centrifugations and redispersed in ethanol.

Host matrix

PVP was chosen as host matrix due to its transparent and non-absorbing properties in the visible range. Furthermore, the pyridil group has strong affinity to metals, such as silver NP [28]. A few microliters of a high-concentrated PVP solution (40 g/l) in ethanol, was added to the washed NP.

Deposition of thin film layers

The substrates were chosen according to the measurements performed afterwards. Indeed, spectrophotometer measurements require a transparent substrate, therefore microscopic glass slides (VWR international) were used. Spectroscopic ellipsometry required a high optical index difference between the substrate and the thin film layer, so that a silicon wafer was chosen. The substrates were cleaned in ultrasonic bath in acetone and ethanol, dried by nitrogen flow and an oxygen plasma. The latter step also increased the wettability of the substrate.

The deposition of the thin film layers was performed by spin coating. The spin coating speed was set to 500 to 1000 rpm, in order to obtain layers of a few hundred micrometers thickness. The deposition technique yields homogeneous thin film layers in the center of the sample, where the optical measurements are performed. Nevertheless, every measurement is repeated at least twice on two different areas to avoid thickness dependent artefacts. Thickness and homogeneity of the thin films were determined by mechanical stylus profilometer (Brucker Decktak XT).

Acknowledgements

Funding: The research was supported by a DGA-MRIS scholarship to Miriam Carlberg and Florent Pourcin.

References

1. Gentile A, Ruffino F, Grimaldi MG. Complex-Morphology Metal-Based Nanostructures: Fabrication, Characterization, and Applications. *Nanomaterials*. 2016;6:110.
2. Daniel M-C, Astruc D. Gold nanoparticles: assembly, supramolecular chemistry, quantum-size-related properties, and applications toward biology, catalysis, and nanotechnology. *Chem. Rev.* 2004;104:293–346.
3. Wang AZ, Langer R, Farokhzad OC. Nanoparticle delivery of cancer drugs. *Annu. Rev. Med.* 2012;63:185–198.

4. Shenashen MA, El-Safty SA, Elshehy EA. Synthesis, Morphological Control, and Properties of Silver Nanoparticles in Potential Applications. Part. Part. Syst. Charact. 2014;31:293–316.
5. de Aberasturi DJ, Serrano-Montes AB, Liz-Marzán LM. Modern Applications of Plasmonic Nanoparticles: From Energy to Health. *Adv. Opt. Mater.* 2015;3:602–17.
6. Otanicar TP, DeJarnette D, Hewakuruppu Y, Taylor RA. Filtering light with nanoparticles: a review of optically selective particles and applications. *Adv. Opt. Photonics.* 2016;8:541–585.
7. García MA. Surface plasmons in metallic nanoparticles: fundamentals and applications. *J. Phys. Appl. Phys.* 2011;44:283001.
8. Jones AR. Light scattering for particle characterization. *Prog. Energy Combust. Sci.* 1999;25:1–53.
9. Khlebtsov NG. Optics and biophotonics of nanoparticles with a plasmon resonance. *Quantum Electron.* 2008;38:504.
10. Schuller JA, Barnard ES, Cai W, Jun YC, White JS, Brongersma ML. Plasmonics for extreme light concentration and manipulation. *Nat. Mater.* 2010;9:193–204.
11. Cushing SK, Wu N. Progress and perspectives of plasmon-enhanced solar energy conversion. *J. Phys. Chem. Lett.* 2016;7:666–675.
12. Akselrod GM, Huang J, Hoang TB, Bowen PT, Su L, Smith DR, et al. Large-Area Metasurface Perfect Absorbers from Visible to Near-Infrared. *Adv. Mater.* 2015;27:8028–8034.
13. Hu C, Liu L, Zhao Z, Chen X, Luo X. Mixed plasmons coupling for expanding the bandwidth of near-perfect absorption at visible frequencies. *Opt. Express.* 2009;17:16745–9.
14. Liu N, Mesch M, Weiss T, Hentschel M, Giessen H. Infrared Perfect Absorber and Its Application As Plasmonic Sensor. *Nano Lett.* 2010;10:2342–8.
15. Hao E, Schatz GC. Electromagnetic fields around silver nanoparticles and dimers. *J. Chem. Phys.* 2004;120:357–366.
16. Arakelyan SM, Veiko VP, Kutrovskaya SV, Kucherik AO, Osipov AV, Vartanyan TA, et al. Reliable and well-controlled synthesis of noble metal nanoparticles by continuous wave laser ablation in different liquids for deposition of thin films with variable optical properties. *J. Nanoparticle Res.* 2016;18:1–12.
17. Mulfinger L, Solomon SD, Bahadory M, Jeyarajasingam AV, Rutkowsky SA, Boritz C. Synthesis and study of silver nanoparticles. *J Chem Educ.* 2007;84:322.
18. Aherne D, Ledwith DM, Gara M, Kelly JM. Optical properties and growth aspects of silver nanoprisms produced by a highly reproducible and rapid synthesis at room temperature. *Adv. Funct. Mater.* 2008;18:2005–2016.
19. Voué M, Dahmouchene N, De Coninck J. Annealing of polymer films with embedded silver nanoparticles: Effect on optical properties. *Thin Solid Films.* 2011;519:2963–2967.
20. Kravets VG, Neubeck S, Grigorenko AN, Kravets AF. Plasmonic blackbody: Strong absorption of light by metal nanoparticles embedded in a dielectric matrix. *Phys. Rev. B.* 2010;81:165401.
21. Sau TK, Rogach AL. Nonspherical noble metal nanoparticles: colloid-chemical synthesis and morphology control. *Adv. Mater.* 2010;22:1781–1804.
22. Zhang J, Langille MR, Mirkin CA. Synthesis of silver nanorods by low energy excitation of spherical plasmonic seeds. *Nano Lett.* 2011;11:2495–2498.
23. Fujiwara H. Spectroscopic ellipsometry: principles and applications [Internet]. John Wiley & Sons; 2007 [cited 2017 Mar 21]. Available from: <https://books.google.fr/books?hl=fr&lr=&id=tTMn0NKcpjsC&oi=fnd&pg=PR7&dq=Sp>

ectroscopic+Ellipsometry:+Principles+and+Applications&ots=NqWTnrQXvO&sig=iOq
pHLDoiH15wSgP_-o51jUWF5Y

24. Tompkins H, Irene EA. Handbook of ellipsometry [Internet]. William Andrew; 2005 [cited 2017 Mar 21]. Available from: https://books.google.fr/books?hl=fr&lr=&id=6PQf1fSzHHEC&oi=fnd&pg=PP1&dq=handbook+of+ellipsometry&ots=_ASgdsfqm3&sig=L_HM89eQKp5BDxrnzupygyL5Wfw
25. Baron A, Iazzolino A, Ehrhardt K, Salmon J-B, Aradian A, Kravets V, et al. Bulk optical metamaterials assembled by microfluidic evaporation. *Opt. Mater. Express*. 2013;3:1792–1797.
26. Zhang H-L, Evans SD, Henderson JR. Spectroscopic Ellipsometric Evaluation of Gold Nanoparticle Thin Films Fabricated Using Layer-by-Layer Self-Assembly. *Adv. Mater*. 2003;15:531–534.
27. Oates TWH, Wormeester H, Arwin H. Characterization of plasmonic effects in thin films and metamaterials using spectroscopic ellipsometry. *Prog. Surf. Sci*. 2011;86:328–376.
28. Malynych S, Luzinov I, Chumanov G. Poly (vinyl pyridine) as a universal surface modifier for immobilization of nanoparticles. *J. Phys. Chem. B*. 2002;106:1280–1285.
29. Wang H, Qiao X, Chen J, Wang X, Ding S. Mechanisms of PVP in the preparation of silver nanoparticles. *Mater. Chem. Phys*. 2005;94:449–453.
30. Shin HS, Yang HJ, Kim SB, Lee MS. Mechanism of growth of colloidal silver nanoparticles stabilized by polyvinyl pyrrolidone in γ -irradiated silver nitrate solution. *J. Colloid Interface Sci*. 2004;274:89–94.
31. Seurin MJ, Gilli JM, Sixou P. Addition d'un polymère "flexible" la polyvinylpyrrolidone à des solutions aqueuses mésomorphes d'un polymère semirigide l'hydroxypropylcellulose. *Eur. Polym. J*. 1983;19:683–690.
32. Moiseev SG. Active Maxwell–Garnett composite with the unit refractive index. *Phys. B Condens. Matter*. 2010;405:3042–3045.
33. Levy O, Stroud D. Maxwell Garnett theory for mixtures of anisotropic inclusions: Application to conducting polymers. *Phys. Rev. B*. 1997;56:8035.
34. Skryabin IL, Radchik AV, Moses P, Smith GB. The consistent application of Maxwell–Garnett effective medium theory to anisotropic composites. *Appl. Phys. Lett*. 1997;70:2221–2223.
35. Weiglhofer WS, Lakhtakia A, Michel B. Maxwell Garnett and Bruggeman formalisms for a particulate composite with bianisotropic host medium. *Microw. Opt. Technol. Lett*. 1997;15:263–266.
36. Stroud D. Generalized effective-medium approach to the conductivity of an inhomogeneous material. *Phys. Rev. B*. 1975;12:3368.
37. Carlberg M, Pourcin F, Margeat O, Le Rouzo J, Berginc G, Sauvage R-M, et al. Optical characterizations of silver nanoprisms embedded in polymer thin film layers. *J. Nanophotonics*. 2017;11:43504–43504.